Supporting Information

Bi_2WO_6 Lead-free Ferroelectrics: Microstructure Design, Polar Behavior and Photovoltaic Performance

Xiang He,[a] Chen Chen,[a] Yunyun Gong,[bc] Huarong Zeng,[bd] and Zhiguo Yi*[abc]

[a.]State Key Laboratory of High Performance Ceramics and Superfine Microstructure, Shanghai Institute of Ceramics, Chinese Academy of Sciences, Shanghai 200050, China

[b.]Center of Materials Science and Optoelectronics Engineering, University of Chinese Academy of Sciences, Beijing 100049, China

[c.]CAS Key Laboratory of Optoelectronic Materials Chemistry and Physics, Fujian Institute of Research on the Structure of Matter, Chinese Academy of Sciences, Fuzhou 350002, China

[d.]CAS Key Laboratory of Inorganic Functional Materials and Devices, Shanghai Institute of Ceramics, Chinese Academy of Sciences, Shanghai 200050, China

*Email: zhiguo@mail.sic.ac.cn

INDEX **Pages**

Table S1. Comparison of main ferroelectric parameters of reported BWO ceramics. S2
Figure S1. SEM and XRD patterns of BWO powders and ceramics. S2
Figure S2. XPS spectra of BWO ceramics. S3
Figure S3. XRD and SEM images of ceramics prepared by ordinary sintering method. S4
Figure S4. UV-visible diffuse reflectance spectra of BWO ceramics. S4
Figure S5. Device configuration for the photovoltaic measurement. S5
Figure S6. Light intensity, wavelength and temperature-dependent V_{oc} and I_{sc}. S5
Figure S7. The reproducibility of I_{sc}. S6
Figure S8. Photoresponse speed analysis. S7

Table S1. Comparison of main ferroelectric parameters of reported BWO ceramics.

Source	P_r (μC/cm^2)	J_p (mA/cm^2)	E_c (kV/cm)	d_{33} (pC/N)	ε	n_r
Zeng T. et al. 2009[1]	16.1	-	37	15±0.2	~50	-
Zeng T. et al. 2015[2]	9.4	-	47	9.2	~80	-
Liao Q. et al. 2017[3]	-	-	-	7	-	-
R-BWO (This work)	10.9	0.25	35.2	9.2	92-115	22.9%
T-BWO (This work)	23.6	0.48	48.5	18.2	120-176	44.5%

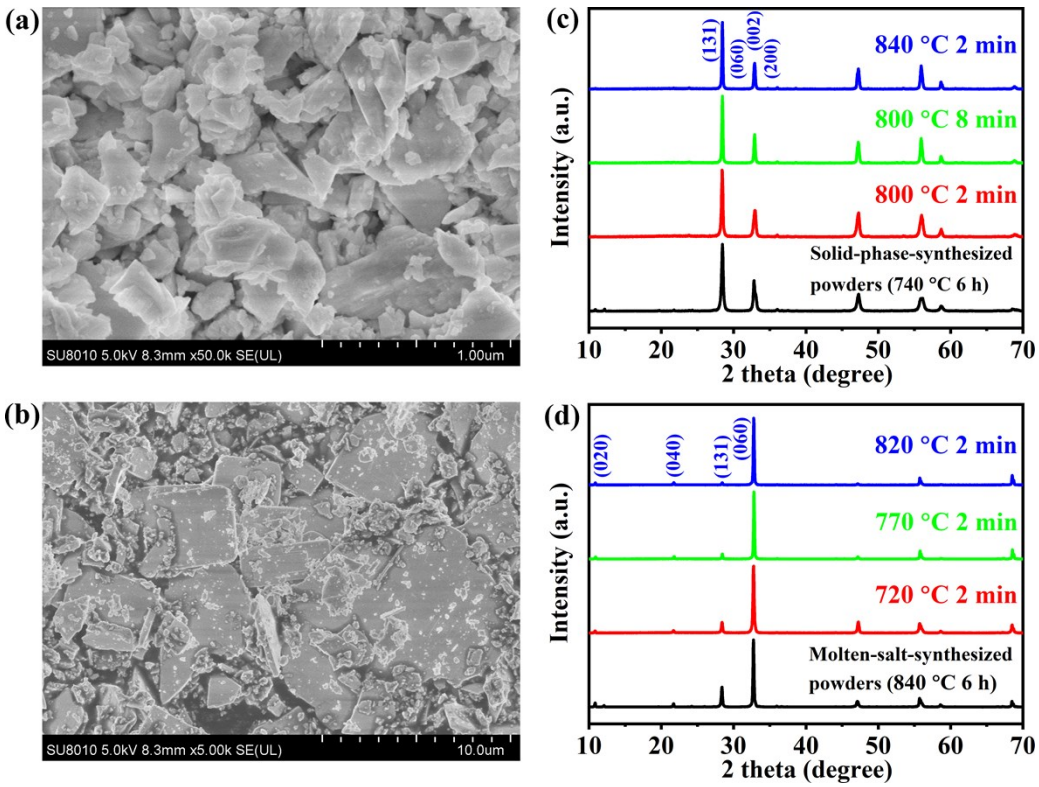

Figure S1. SEM images and XRD patterns of non-plate-like (a,c) and plate-like (b,d) Bi_2WO_6 (BWO) powders, where the plate-like powders exhibit distinct (060) orientation. Besides, the XRD patterns of the BWO ceramics sintered at different temperatures with non-plate-like and plate-like powders are shown in (c) and (d), respectively.

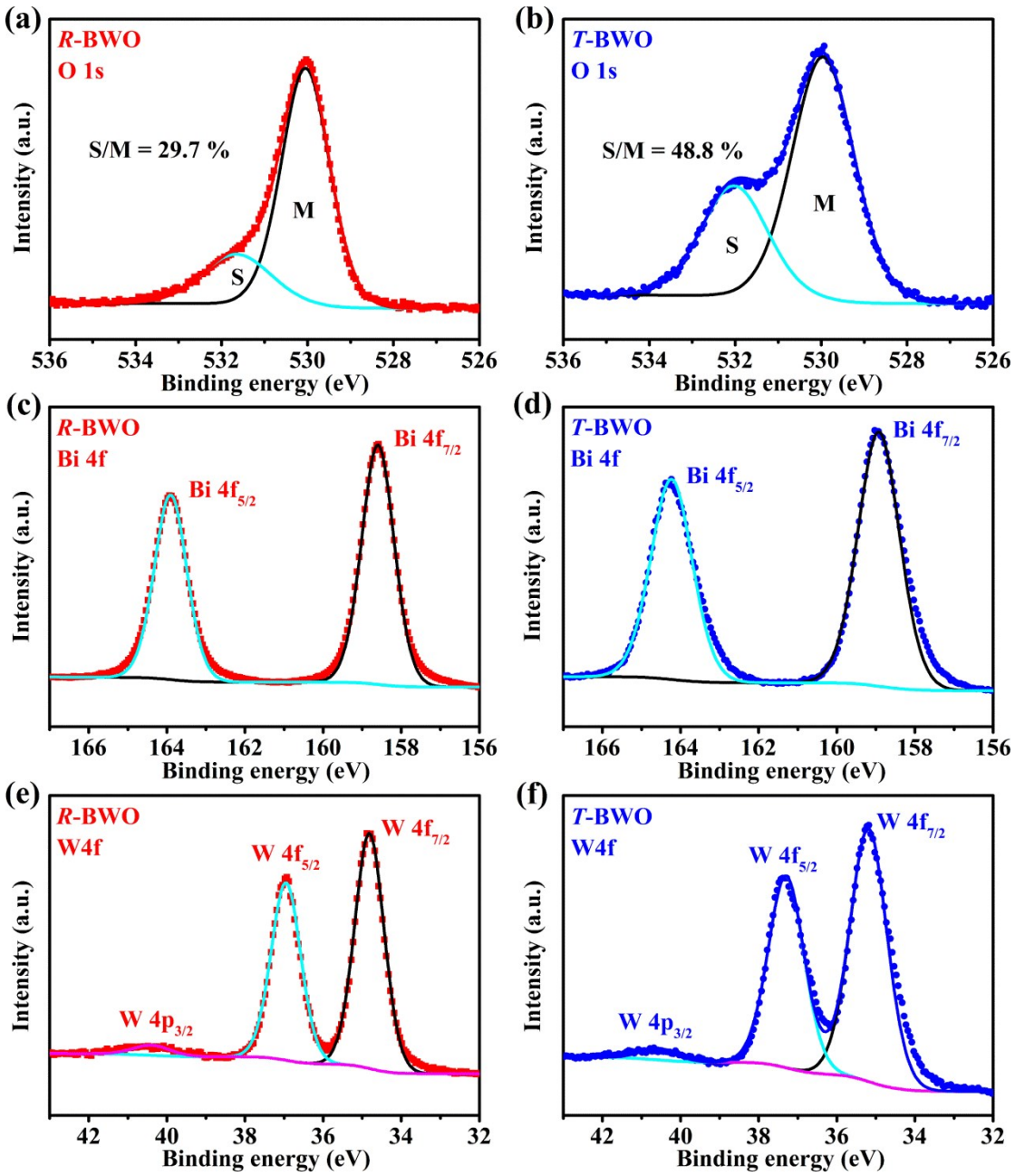

Figure S2. The X-ray photoelectron spectra (XPS) of grain randomly oriented BWO ceramics (*R*-BWO) and grain textured BWO ceramics (*T*-BWO). The binding energies in the spectra were calibrated using that of C 1s (284.62 eV). All the measured peaks (O 1s, Bi 4f, W 4f) are consistent with the previous reports.[4-6] Besides, the O 1s peaks are composed of oxygen vacancy (531.4 eV, S) and lattice oxygen (529.4 eV, M).[7] Therefore, *T*-BWO ceramic contains more oxygen vacancies than *R*-BWO.

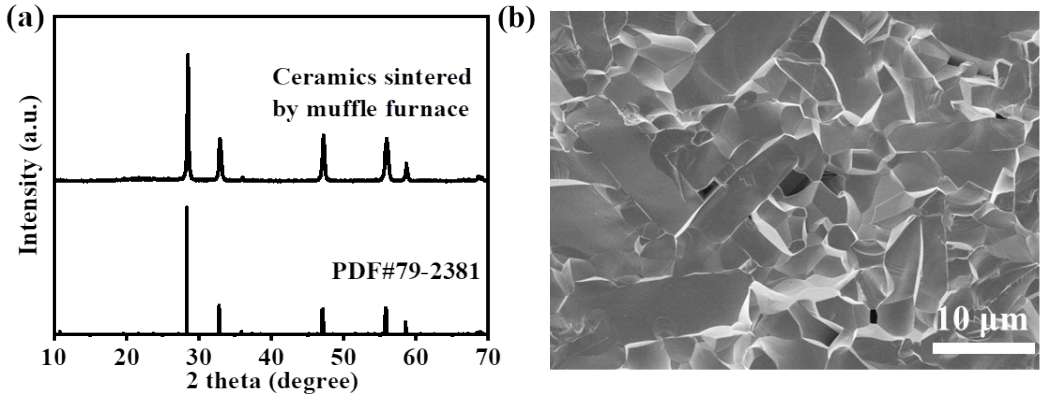

Figure S3. (a) XRD pattern and (b) SEM image of BWO ceramics prepared by conventional solid state sintering method.

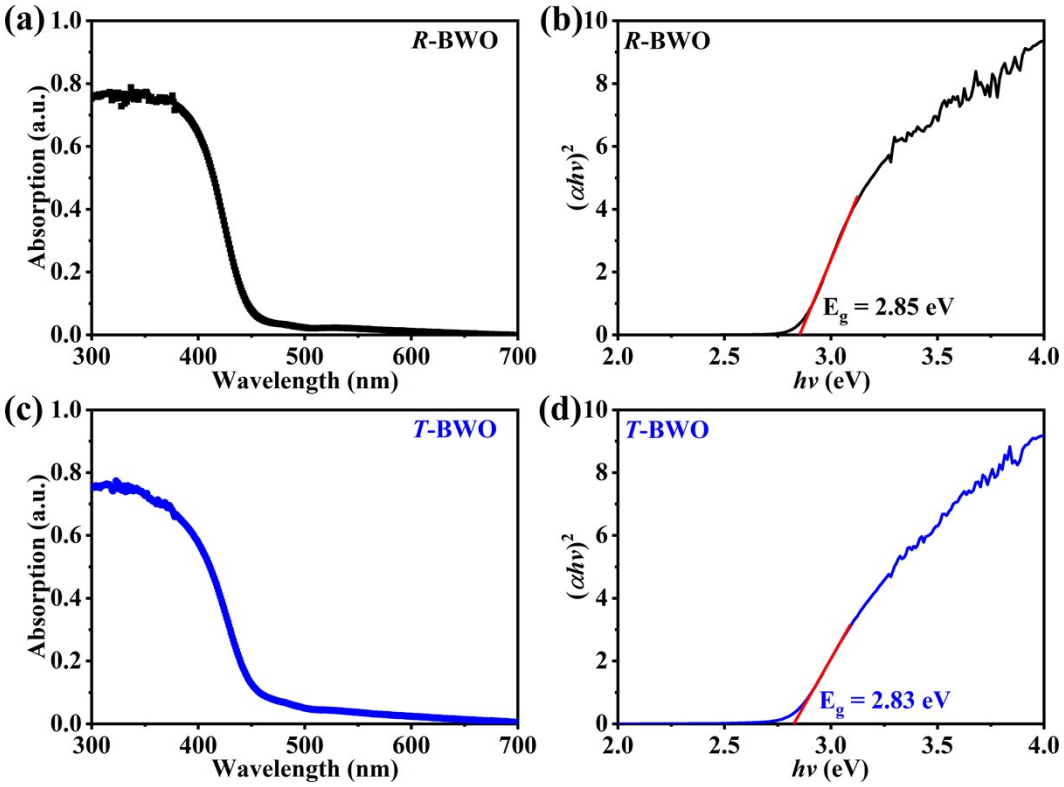

Figure S4. (a,c) UV-visible diffuse reflectance spectra and (b,d) Tauc plots of *R*-BWO (a,b) and *T*-BWO (c,d). The bandgap (E_g) values are deduced by using Tauc equation: $\alpha h\nu = A(h\nu - E_g)^{n/2}$, where α, $h\nu$, A are absorption coefficient, incident light energy, and proportionality constant, respectively.[8] In the equation, n decides the characteristics of the transition in a semiconductor (n = 1, direct absorption; n = 4, indirect absorption). The bandgaps of *R*-BWO and *T*-BWO were calculated to be 2.85 and 2.83 eV, respectively.

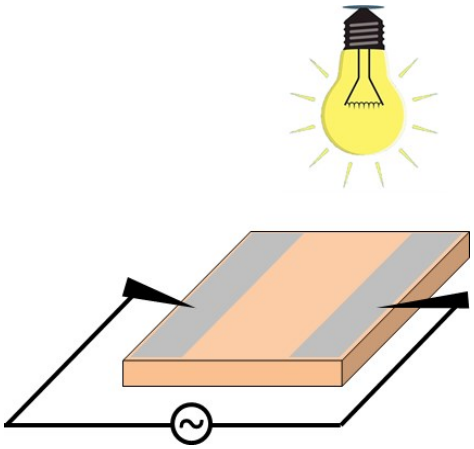

Figure S5. Device configuration for the photovoltaic measurement. The devices are fabricated by depositing two parallel gold (Au) electrodes on one facet of the random/textured BWO ceramic plates (8 mm × 7.5 mm × 0.2 mm) with the same electrode spacing of ~250 μm. The photovoltaic devices were placed in a Linkam thermal stage to control the temperature, and then current-voltage curves were collected by a Keithley 6517B electrometer. A 405 nm laser and a 300 W Xe lamp were used as light source. The monochromatic light in the range of 400 to 550 nm were obtained by inserting band pass filters in between the sample and the Xe lamp.

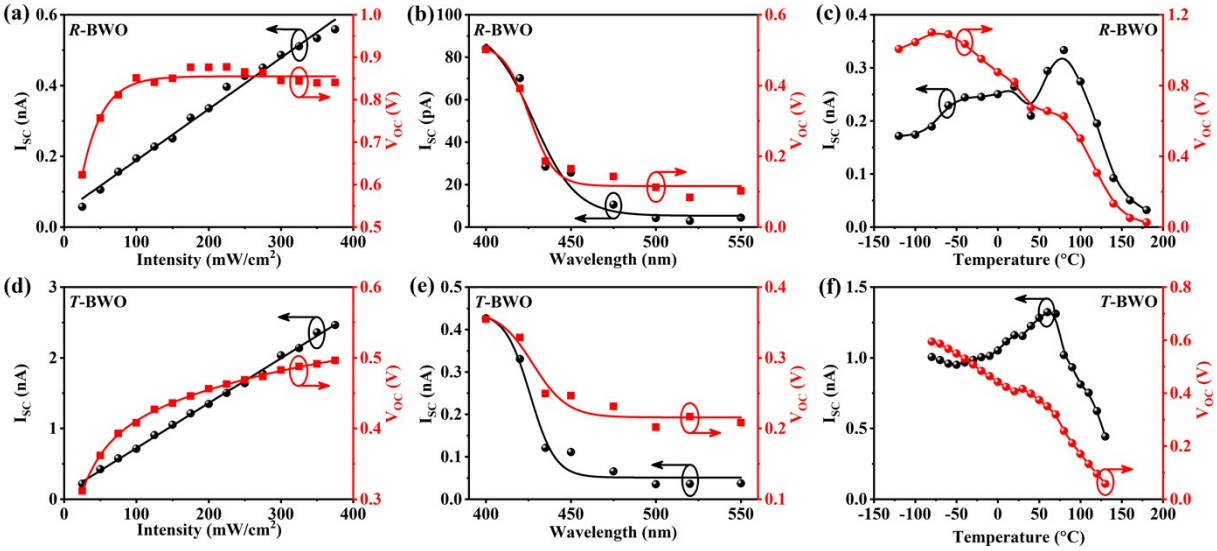

Figure S6. Short circuit current (I_{sc}) and open circuit voltage (V_{oc}) as function of (a,d) light intensity under the illumination of 405 nm laser, (b,e) wavelength with fixed light intensity of 200 mW/cm^2, and (c,f) temperature under the illumination of 200 mW/cm^2 and 405 nm laser for (a,b,c) positively poled *R*-BWO and (d,e,f) positively poled *T*-BWO ceramics, respectively.

The V_{oc} and I_{sc} of poled BWO ceramics are strongly light intensity, wavelength and temperature dependent. Figure S6a and S6d show the light intensity dependence of I_{sc} (absolute value) and V_{oc} for the positively poled *R*-BWO and *T*-BWO photovoltaic devices,

respectively. With the increase of light intensity from 0 to 375 mW/cm^2, the I_{sc} is observed to increase almost linearly for both samples, whereas the V_{oc} gradually saturates at high illumination intensity. According to the equation $V_{oc} = J_s d/(\sigma_d + \sigma_{ph})$, where J_s is the photoinduced current, d is the distance between two electrodes, σ_d and σ_{ph} are the dark conductivity and photo conductivity,[9,10] both J_s and σ_{ph} are positively related to the light intensity, which normally leads to the stability of V_{oc} to some extent. In addition, as decreasing the wavelength of the incident light from 550 nm to 400 nm (Figure S6b and S6e), the V_{oc} and I_{sc} of *R*-BWO and *T*-BWO devices start to increase significantly around 450 nm, closely corresponding to the band gap of BWO materials (2.8 eV). Therefore, 405 nm laser, above band gap, is suitable to evaluate the photoelectric performance of BWO ceramics as the incident light source. The temperature dependence of I_{sc} and V_{oc} for *R*-BWO ceramics shows a similar behavior with that of *T*-BWO ceramics. As shown in Figure S6c and S6f, the highest I_{sc} is reached at 75 °C, but the V_{oc} decreases monotonously with the increasing of the temperature for both random and textured BWO ceramic devices, which should be ascribed to the reduced carrier mobility and enhanced charge recombination rate.

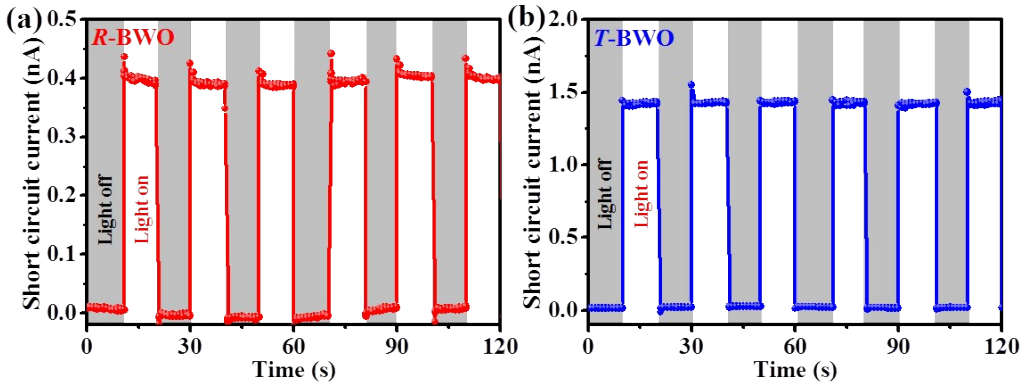

Figure S7. Time dependence of short circuit current with 405 nm laser on/off cycles under a constant light intensity of 200 mW/cm^2.

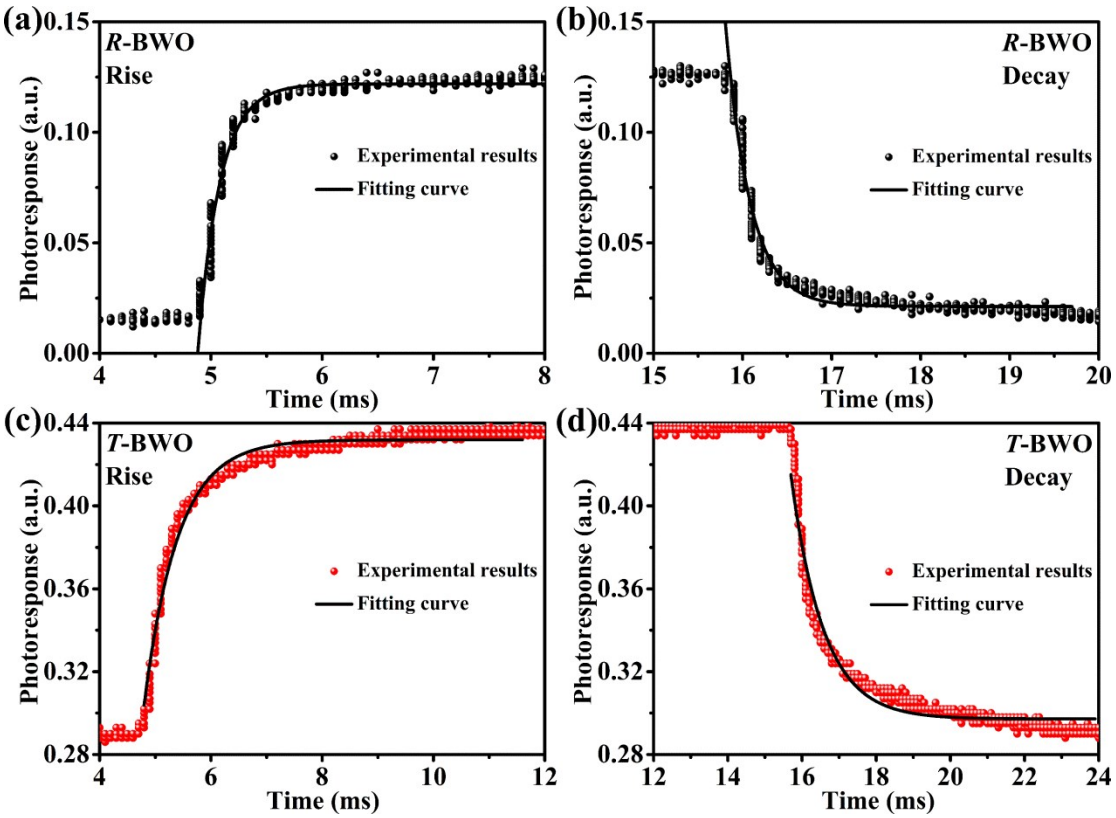

Figure S8. Photoresponse speed analysis of the *R*-BWO (a,b) and *T*-BWO (c,d) ceramics during light on/off switching: (a,c) Enlarged rising and (b,d) decaying process.

References

[1] T. Zeng, H. Yan, H. Ning, J. Zeng and M. J. Reece, *J. Am. Ceram. Soc.*, 2009, **92**, 3108-3110.

[2] T. Zeng, X. Yu, S. Hui, Z. Zhou and X. Dong, *Mater. Res. Bull.*, 2015, **68**, 271-275.

[3] Q. Liao, L. Zheng, Z. An, H. Huang, C. Yan, L. Qin, L. Wang and S. Peng, *J. Alloys Compd.*, 2017, **692**, 454-459.

[4] M. S. Gui, W. D. Zhang, Q. X. Su and C. H. Chen, *J. Solid State Chem.*, 2011, **184**, 1977-1982.

[5] A. Kania, E. Talik, M. Szubka, W. Ryba-Romanowski, A. Niewiadomski, S. Miga and M. Pawlik, *J. Alloys Compd.*, 2016, **654**, 467-474.

[6] R. Tang, H. Su, Y. Sun, X. Zhang, L. Li, C. Liu, B. Wang, S. Zeng and D. Sun, *Nanoscale Res. Lett.*, 2016, **11**, 126.

[7] H. Liu, J. Chen, Y. Ren, L. Zhang, Z. Pan, L. Fan and X. Xing, *Adv. Electron. Mater.*, 2015, **1**, 1400051.

[8] J. Tauc, A. Menth and D. L. Wood, *Phys. Rev. Lett.*, 1970, **25**, 749.

[9] V. M. Fridkin, *Crystallogr. Rep.*, 2001, **46**, 654-658.

[10] A. Bhatnagar, A. R. Chaudhuri, Y. H. Kim, D. Hesse and M. Alexe, *Nat. Commun.*, 2013, **4**, 2835.